REPORT DOCUMENTATION PAGE

Form Approved
OMB No. 0704-0188

1. REPORT DATE *(DD-MM-YYYY)*	2. REPORT TYPE	3. DATES COVERED *(From - To)*
02-03-2009	Final report	3/15/2006-11/30/2008

4. TITLE AND SUBTITLE
Use of the CSA to calculate phase diagrams and coherent inter-phase boundary energies of multi-component Nickel-based alloys

5a. CONTRACT NUMBER

5b. GRANT NUMBER
FA9550-06-1-0229

5c. PROGRAM ELEMENT NUMBER
None

6. AUTHOR(S)
Chuan Zhang, Jun Zhu, Weisheng Cao and Y. Austin Chang

5d. PROJECT NUMBER
FA9550-06-0229

5e. TASK NUMBER
None

5f. WORK UNIT NUMBER
None

7. PERFORMING ORGANIZATION NAME(S) AND ADDRESS(ES)
Department of Materials Science and Engineering
University of Wisconsin - Madison
1509 University Avenue
Madison, WI-53706

8. PERFORMING ORGANIZATION REPORT NUMBER
None

9. SPONSORING / MONITORING AGENCY NAME(S) AND ADDRESS(ES)
The Air Force Office of Scientific Research (AFOSR)
Arlington, VA

10. SPONSOR/MONITOR'S ACRONYM(S)
AFOSR

11. SPONSOR/MONITOR'S REPORT NUMBER(S)
None AFRL-AFOSR-VA-TR-2016-0060

12. DISTRIBUTION / AVAILABILITY STATEMENT
Distribution A - Approved for public release

13. SUPPLEMENTARY NOTES
None

14. ABSTRACT
Computational thermodynamics coupled with key experiments rapidly accelerate the development of multi-component phase diagrams. These diagrams act as road maps for selecting alloy compositions and processing parameters for solidification and heat treatments in order to achieve desirable performance such as their mechanical properties and oxidation-resistance. In this report, we obtain a thermodynamic description of Ni-Al-Cr-Pt via extrapolation from descriptions of the constituent binaries and those of key ternaries. The reliability of the description obtained was validated using experimental results obtained in this study. In addition, we also completed a description of Ni-Al-Cr-Ru initiated in an earlier program. We also demonstrated that the method used by us in calculating the inter-phase boundary (IPB) energies between γ(fcc) and $\gamma'(L1_2)$ in binary Ni-Al [2006Cao] is able to calculate those between γ and γ' in ternary Ni-Al-Cr [2006Cao1]. We can thus conclude that this method can be used to calculate IPB energies between γ and γ' in multi-component Ni-base alloys.

15. SUBJECT TERMS
multi-component phase equilibria, thermodynamics, interphase boundary energies

16. SECURITY CLASSIFICATION OF: None			17. LIMITATION OF ABSTRACT	18. NUMBER OF PAGES	19a. NAME OF RESPONSIBLE PERSON
a. REPORT	b. ABSTRACT	c. THIS PAGE	SAR	19	Y Austin Chang
					19b. TELEPHONE NUMBER *(include area code)* 608-262-0389

FINAL TECHNICAL REPORT

Use of the CSA to calculate phase diagrams and coherent Nickel-based alloys

AFOSR GRANT FA9550-06-1-0229

Department of Materials Science and Engineering

Chuan Zhang, Jun Zhu, & Weisheng Cao,

University of Wisconsin Madison

1509 University Avenue

Madison, Wi 53706

Y. Austin Chang

Use of the CSA to Calculate Phase Diagrams and Coherent Inter-phase Boundary Energies of Multi-Component Nickel-based Alloys

Project Summary

The fundamental interest in the technologically important Ni-rich alloys is that they consist of the fcc phase (A1), referred to as γ, and one of its ordered forms ($L1_2$), referred to as γ'. Since the Bragg-Williams model used in the traditional Calphad approach is known to have difficulties in giving a satisfactory description of the thermodynamics of the fcc phases, it is essential to have a suitable and computationally efficient model to describe the thermodynamics of these phases, i.e., the fcc phase, an ordered fcc phase, $L1_2$, with a stoichiometry of 0.75:0.25, and another ordered fcc phase, $L1_0$, with a stoichiometry of 0.5:0.5.

We have recently extended the use of the cluster/site approximation (CSA) to describe the fcc phases from binary Ni-Al alloys to ternaries for phase diagram calculation. Subsequent to showing that the CSA-calculated coherent Cu-Ag-Au phase diagrams are essentially the same as the CVM-calculated ones [80Kik], we extended the use of the CSA to calculate Ni-Al-Cr phase diagrams. The agreement between the CSA-calculated stable phase diagrams and the experimental data is as good as that obtained by the traditional Calphad approach [98Hua] but *with fewer parameters*. More importantly, the topological features of the CSA-calculated metastable phase diagrams, such as isotherms and isopleths involving only the fcc phases or the fcc and liquid phases, are what one expects, as has been demonstrated previously for the binary Ni-Al alloys [2003Zha]. In view of the computational advantage of the CSA versus the CVM and the capability of the CSA in describing the thermodynamics of the fcc phases satisfactorily, we have recently experimented with the use of the CSA to calculate coherent inter-phase boundary (IPB) energies. Following the approach of Kikuchi and Cahn [95Kik], we have calculated the coherent IPB energies between the fcc (A1) and $L1_2$ phases in prototype Cu-Au alloys as a function of temperature using the CSA instead of the CVM. The CSA-calculated IPB energies are in accord with the CVM-calculated values. We next extended this approach to calculate IBP energies between γ and γ' in Ni-Al and those between Al and Al_3Li in Al-Li. The CSA-calculated IPB energies between γ and γ' are in accord with the experimental data [95Ard] and those obtained from "first principles" calculations together with the cluster expansion method coupled with Monte Carlo calculations [2004Woo]. Similarly, the results obtained between Al and Al_3Li also agree with the experimental data [91Hoy, 84Bau] and those calculated from "first principles" coupled with the CVM [96Ast].

Accordingly, we propose to carry out the following studies for a three-year period from 5/1/06 to 4/30/09: (1a) to extend the CSA-phase diagram calculation to a quaternary system such as Ni-Al-Cr-Re, (1b) to use a combined computational/experimental approach to obtain a thermodynamic description of Ni-Al-Pt, (1c) to obtain a thermodynamic description of the quaternary Ni-Al-Cr-Pt by extrapolation with experimental validation, and (2) to extend the use of CSA to calculate IPB energies between γ and γ' in ternary Ni alloys such as Ni-Al-Cr. In addition to advancing the Calphad methodology to calculate multicomponent phase diagrams for alloys containing the fcc phases using the CSA and developing a methodology to calculate coherent IPB energies also using the CSA, the proposed study will generate thermodynamic descriptions and IPB energies between γ and γ' of the technologically important Ni-based alloys. These data are essential for predicting microstructure evolution during the processing of these alloys and ultimately their mechanical behaviors.

1.0 Introduction

Advancement of modern turbine engine demands development of new materials as well as improvement of existing materials to withstand the harsh environments of high temperature and cyclic stress. The traditional approach relying on pure experimentation and ingenious intuition of materials scientists and engineers to achieve this goal is no longer a viable option due to the constraint of available resources. It takes too long, costs too much, and is challenging to obtain resources to undertake this task. However, with recent advances made in computational materials science and engineering, it is likely that we will be able to achieve this goal in the not distant future by using computational tools integrated with limited amount of experimentation. In this proposed study, we focus on the use of computational thermodynamics, specifically the Calphad approach, to calculate multicomponent phase diagrams and coherent inter-phase boundary (IPB) energies of nickel-based alloys. In the Calphad approach, the Gibbs energy of each phase is described by a phenomenological thermodynamic model. The thermodynamic model parameters of alloy phases in the lower order systems, *viz.* normally binaries and ternaries, are obtained in terms of the available thermodynamic and phase equilibrium data. Since phase equilibria are governed by the relative Gibbs energies of the phases involved, the accuracy of the Gibbs energies obtained either experimentally or the "first principle" calculated values at 0K is often insufficient to differentiate which of the possible phase equilibria is the stable one. This means that thermodynamic values combining phase equilibrium data are needed to obtain a reliable thermodynamic description. The term "thermodynamic description" denotes that thermodynamic models with parameters of all the phases for the system in question are available. When thermodynamic descriptions of the constituent binaries and ternaries of a multicomponent system are available, we can in *many cases*, obtain a thermodynamic description of this multicomponent system by extrapolation based on the model parameters of phases in the lower order systems [89Cho]. This significant achievement makes it possible to calculate multicomponent phase diagrams for basic research in an allied field and technological applications.

Two of the major phases in the Ni-based superalloys are the Ni solid solution with the fcc structure, referred to as γ and the Ni_3Al solution with the $L1_2$ structure, an ordered form of the fcc structure. This phase is normally referred to as γ'. In the traditional Calphad approach, the Bragg-Williams model is used to describe the thermodynamics of ordered phases [86And, 2004Cha]. However, since this model is formulated based on the point approximation and does not take into account the existence of short-range ordering (SRO) in alloys at high temperatures, it cannot satisfactorily account for the thermodynamics of order/disorder transformations such as γ'/γ [38Sho, 79deF, 94DeF]. Thus, the current approach does not lend confidence when extrapolating the thermodynamic descriptions of lower order systems to multicomponent alloys when ordered phases are involved, such as the technologically important Ni-based alloys. Although it is known that the cluster variation method (CVM) is able to describe the thermodynamics of order/disorder transformation [51Kik, 74Kik, 78San], it is computationally intensive. On the other hand, the cluster/site approximation (CSA) also considers the existence of SRO but computationally less demanding [96Oat, 99Oat]. We had shown previously the adequacy of the CSA for describing the thermodynamics of fcc-base (and hcp-base) phases in several alloys, i.e. Cu-Au, Cd-Mg and Ni-Al [99Oat, 2001Zha, 2003Zha, 2004Cha]. More recently, we extended the CSA first to the prototype ternary Cu-Ag-Au and then to the Ni-Al-Cr system. The CSA-calculated phase diagrams of the former are the same as the CVM-calculated ones. For the later ternary, the agreement between the

CSA-calculated stable diagrams and experimental data is as good as that obtained by the traditional Calphad approach [98Hua] but *with fewer parameters*. The CSA-calculated metastable phase diagrams are what one expected [2005Cao1].

We next experimented with the use of the CSA to calculate the coherent IPB energies between the fcc (A1) and $L1_2$ phases for prototype Cu-Au and then those for Ni-Al and Al-Li. The CSA-calculated coherent IPB energies are in accord with the CVM-calculated values for prototype binaries [79Kik, 96Ast1]. Moreover the CSA-calculated coherent IPB energies between γ and γ' in Ni-Al and between (Al) and metastable Al_3Li are also in accord with available experimental data [95Ard, 91Hoy] and values obtained from "first principles" calculations either with the CVM or cluster expansion method coupled with Monte Carlo calculations [96Ast, 2004Woo].

On the basis of the success of using the CSA to calculate binary Ni-Al and ternary Ni-Al-Cr phase diagrams as well as IPB energies between the fcc (A1) and $L1_2$ phases in prototype Cu-Au and two real binary alloys Al-Al_3Li and Ni-Al, we propose to carry out the following studies: (1a) to extend the CSA-phase diagram calculation to a quaternary system such as Ni-Al-Cr-Re, (1b) to use a combined computational/experimental approach to obtain a thermodynamic description of Ni-Al-Pt, (1c) to obtain a thermodynamic description of the quaternary Ni-Al-Cr-Pt by extrapolation with experimental validation and (2) to extend the use of the CSA to calculate IPB energies between γ and γ' in a ternary Ni alloy such as Ni-Al-Cr. In addition to advancing the Calphad methodology to calculate multicomponent phase diagrams for alloys containing the fcc phases using the CSA and developing a methodology to calculate coherent IPB energies also using the CSA, the proposed study will generate thermodynamic descriptions and IPB energies between γ and γ' of the technologically important Ni-based alloys. These data are essential for predicting microstructure evolution during the processing of these alloys and ultimately their mechanical behaviors.

In the following we will present in **Section 2.0 Technical Discussion, Section 3.0 Proposed Study, Section 4.0 Experimental Facilities, Section 5.0 References Cited, Section 6.0 The Principal Investigator and Section 7.0 Proposed Budget.**

2.0 Technical Discussion

2.1 The Application of the CSA to fcc Phases in Multi-component Nickel-based Alloys

As noted in **Section 1.0**, the Bragg-Williams model used in the traditional Calphad approach is not able to describe the thermodynamics of the fcc phases due to the neglect of short-range ordering (SRO) in alloys at high temperatures [38Sho, 79deF, 94DeF]. On the other hand, the cluster variation method (CVM) is capable [51Kik, 74Kik, 78San] but is computationally intensive. We had shown previously the adequacy of the CSA for describing the thermodynamics of fcc-base (and hcp-base) phases in Cu-Au, Cd-Mg and Ni-Al [99Oat, 2001Zha, 2003Zha, 2004Cha]. More recently, we successfully extended the use of CSA first to the prototype ternary Cu-Ag-Au and then to the Ni-Al-Cr systems. The results obtained for the former were presented by W. Cao at the 2005 TMS Annual Meeting and have been published [05Cao]. A manuscript describing the results obtained for Ni-Al-Cr has been submitted to Acta Mater. for publication [05Cao1]. Prior to presenting the research results,

we will first introduce the basic thermodynamic formulation for the CSA [04Cha, 05Cao] as given below.

The Gibbs energy of the fcc-base phases consisting of two terms is given below [98Sun],

$$G = G^{CI}(x_p) + G^{CD}(y_p^{(i)}) \qquad (1)$$

The quantity G^{CI} is the configurational independent term that depends only on the mole fractions of the component elements, i.e. x_p, in the alloys but not on the details of the sublattice species occupation $y_p^{(i)}$. It is used to account for such quantities as excess elastic energies due to atomic size mismatch, changing cell relaxation as well as other excess excitation contributions. The term G^{CD} is the configuration dependent term and is a function of the distribution of the species $y_p^{(i)}$ on the respective sublattices. For the configuration independent Gibbs energy G^{CI}, we use the Redlich-Kister equation [48Red]. The term for G^{CD} according to the CSA [96Oat, 99Oat, 2001Zha1, 2003Zha] is

$$G^{CD} = \zeta RT\left(\sum_{p}^{C-1}\sum_{i=1}^{n} y_p^{(i)}\mu_p^{(i)} - \ln\varphi\right) - (n\zeta - 1)RT\sum_{p}^{C}\sum_{i=1}^{n} f_i y_p^{(i)} \ln y_p^{(i)} \qquad (2)$$

where ζ is the number of non-interfering clusters per site in the original CSA model [e.g., 47Yan] but can be treated as a parameter in developing a thermodynamic description of an alloy system, f_i are the sublattice fractions, n is the size of the cluster, and $y_p^{(i)}$, defined earlier, are the species fractions of component p on sublattice i. The $\mu_p^{(i)}$s are the Lagrangian multipliers for the mass balance constraints in the Gibbs energy minimization and, physically, are related to the species chemical potentials of the lattice gas particles on the sublattice i. The cluster partition function, ϕ is defined as,

$$\phi = \left(\sum_{j=1}^{C^n} \exp[(\sum_{i=1}^{n}\mu_p^{(i)})_j - \varepsilon_j]\right) \qquad (3)$$

where ε_j is the cluster energy of a j-type cluster. The cluster energy can be obtained from the pair exchange energies, W, between components i and j.

For the prototype Cu-Ag-Au system, we compared the CSA-calculated coherent phase diagrams with the CVM-calculated ones by Kikuchi et al. [80Kik]. In other words, the G^{CI} term in Eq. (1) is taken to be zero. The CSA-calculated isotherms at high temperatures are in accord with the CVM-calculated ones [80Kik]. However, there is a distinct difference in the CSA-calculated isotherm at 240°C with the CVM-calculated one as shown in Figs. 1(a) and (b). As shown in these two figures, while the CSA-calculated isotherm shows the existence of an island of the (Cu, Ag)Au_3 ($L1_2$) phase within the single-phase field of fcc α-(Au, Cu, Ag), the CVM-calculated isotherm shows the absence of such an island! Prof. C. Colinet of LTPCM-ENSEEG, Saint Martin d'Heres, France subsequently re-calculated this isotherm using the CVM and indeed found the existence of the $L1_2$ phase in the Au-rich corner as shown in Fig. 1(b). In the original CVM calculation, it was necessary to know the existence

of this $L1_2$ phase in the Au-rich corner so as to estimate initial values to calculate the compositional stability of this phase. On the other hand, we use the Pandat software, which is able to automatically find the lowest Gibbs energy and thus obtain the most stable phase state automatically [2003Che, 2002Che, 2001Che]. As noted above, ζ is the number of non-

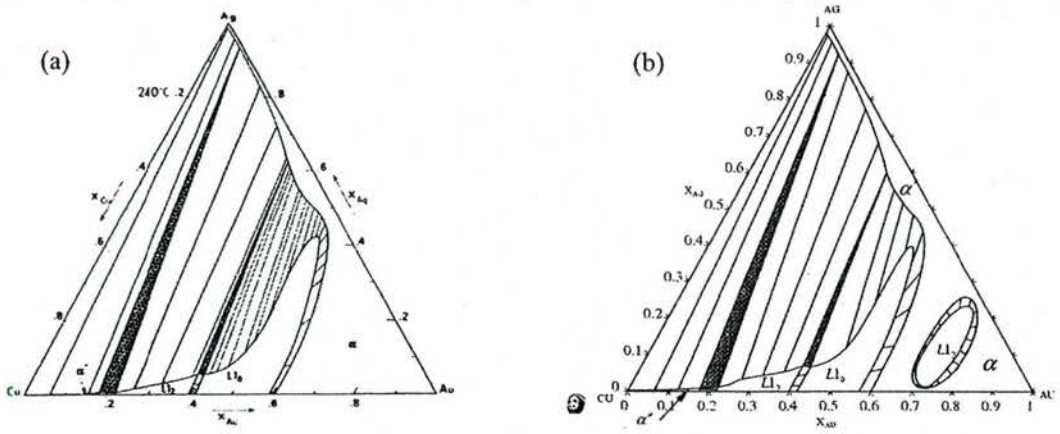

Figure 1 Calculated isotherms of Cu-Ag-Au at 240°C: (a) CVM [80Kik] and (b) CSA

interfering clusters per site in the original CSA model (Eq. 2). A value of $\zeta = 1.42$ was used for all three constituent binaries of Cu-Ag-Au [2005Cao], which should be unity for an fcc structure. It is also noteworthy to point out that values of the pair exchange energies used in the CSA are, on the average, within 5% of those used in the CVM.

Subsequent to successfully extending the CSA from binaries to calculate ternary phase diagrams for the Cu-Ag-Au system, we began to apply this approximation to the fcc phases in the Ni-Al-Cr ternary system. Since the fcc phases in Ni-Al had already been modeled using the CSA by Zhang et al. [2003Zha], we adopted their description. The model parameters for the fcc phases in the other two constituent binaries were obtained from the experimental data

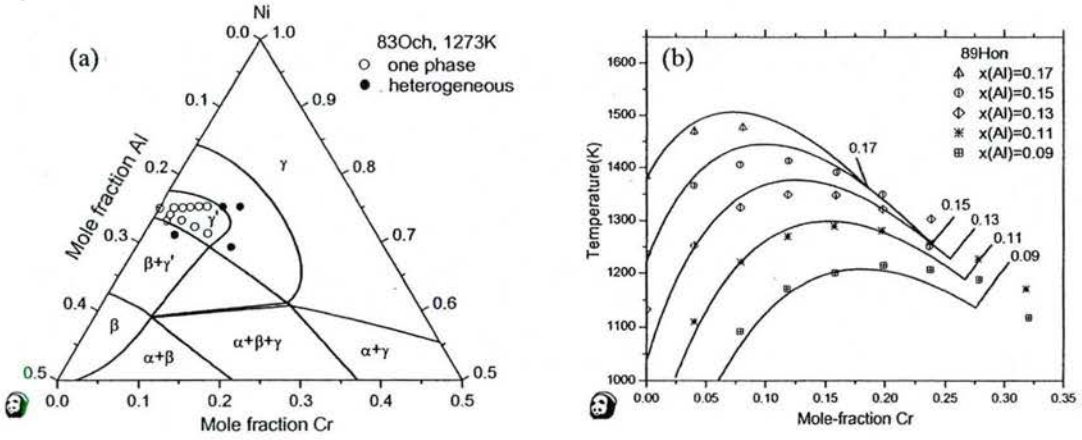

Figure 2 Comparison of calculation with experimental data of Ni-Al-Cr: (a) 1,273K (1,000°C) isothermal section and (b) the γ-solvus at constant values of Al

assessed in the literature [2005Cao1, 98Hua]. Figures 2(a) and (b) show the CSA-calculated isotherm of Ni-Al-Cr at 1273K and the CSA-calculated γ-solvus curves as a function of temperature along with experimental data. These γ-solvus curves were calculated at constant values of the mole fraction of Al varying from 0.09 to 0.17. The calculated phase boundaries as shown in Fig. 2(a) are consistent with the experimental data of Ochiai et al. [83Och] and

the calculated solvus of the γ-phase shown in Fig. 2(b) is in accord with the data of Hong et al. [89Hon]. Many other comparisons between calculation and experimental data were made and the agreement is similar to those shown in Fig. 2(a) and (b) but not presented here.

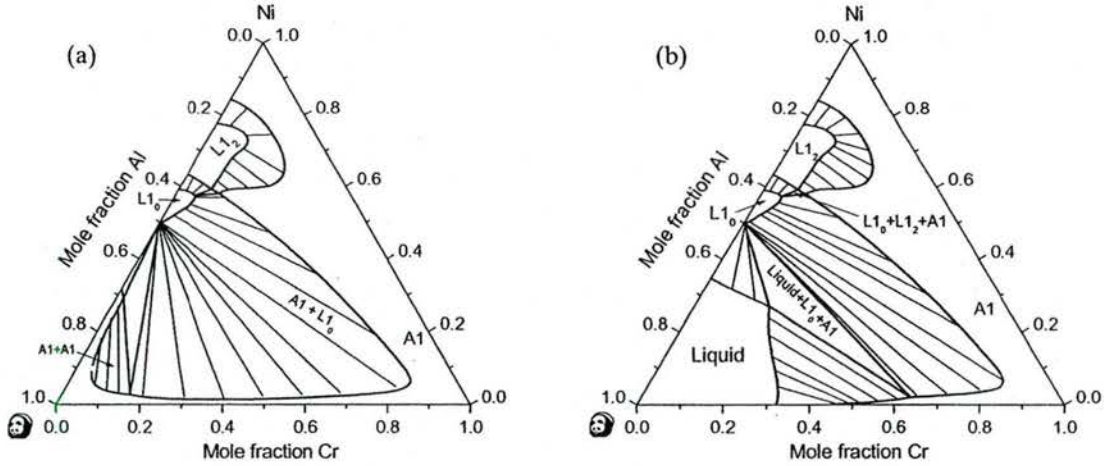

Figure 3 Calculated metastable isotherms at 1273K (1000°C): (a) Phase equilibria involving only the fcc phases and (b) Phase equilibria involving only the fcc and the liquid phases.

The important question is, can we calculate metastable phase diagrams that are topologically correct using the thermodynamic models developed for each phase in terms of stable ternary phase equilibrium data as well as the binary thermodynamic descriptions? If we can, then the calculated metastable phase diagram can be used to study phase transformations and are likely to motivate researchers to synthesize metastable phases with desirable properties via novel experimental techniques. As shown in Fig. 3(a, b), the calculated $\gamma + \gamma'$ (or $A1 + L1_2$) phase equilibria in the Ni-rich corner are nearly the same, as anticipated, since they correspond to the stable equilibria as can be seen from Fig. 2(a). Moreover, the calculated metastable phase equilibria away from the stable region, although different in these two diagrams, are consistent with the phase rule. In other words, the extensions of the phase boundaries to the metastable region show the existence of two-phase fields of $L1_2 + L1_0$, $A1 + L1_0$ as well as

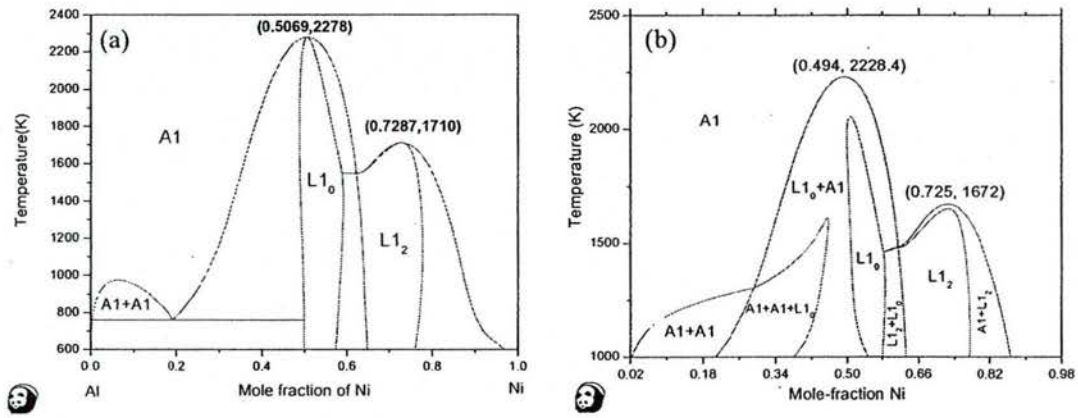

Figure 4 CSA-calculated metastable fcc(A1) phase diagrams: (a) Binary Ni-Al [2003Zha] and (b) An isopleth of Ni-Al-Cr with constant value of 2 at % Cr [2005Cao1]

immiscibility of the A1 phase with the corresponding three-phase field toward the Al-rich corner. It is worth noting that Zhang et al. [2003Zha] had shown an immiscibility gap occurring in the A1 phase in the Al-rich side of the calculated metastable fcc Al-Ni binary

diagram as shown in Fig. 4(a). It is noteworthy to point out that *the topological features given in Fig. 4(a) are the same as those obtained from "first principle" calculations coupled with the CVM* [e.g. 92Pas]. To the best of our knowledge none of the descriptions of Ni-Al obtained from the Calphad approach is able to do so [2003Zha, 2004Cha]. For Fig. 3(b), the liquid phase appears in the Al-rich corner with corresponding two- and three-phase fields involving the liquid phase. It is interesting also to compare the calculated metastable fcc isopleth with 2 at% Cr with that of Ni-Al [2003Zha] as shown in Fig. 4. Figure 4(a) shows that the A1(fcc) phase is stable at high temperatures. With decreasing temperature, the $L1_0$ appears at 50 at% Ni, the $L1_2$ phase at 75 at% Ni, and two A1 (fcc) phases toward the Al-rich side. The calculated isopleth with 2 at% Cr shown in Fig. 4(b) has similar features except (i) a three-phase field of A1 + A1 + $L1_0$ appears between the 2 two-phase fields of A1 + A1 and A1 + $L1_0$ and (ii) both the $L1_0$ and $L1_2$ phases no longer melt congruently as should be the case. These results are expected since a binary invariant such as the binary monotectoid, A1 + A1 + $L1_0$, becomes a tie-triangle in the ternary region over a range of temperatures. Of course there is also another three-phase equilibrium of A1 + $L1_0$ + $L1_2$ also shown in this diagram at ~ 1470K and ~ 60 at% Ni. Many other diagrams could be calculated such as the liquidus projection of the metastable phase diagram involving only the fcc (A1) and liquid phases. Additional metastable diagrams were presented in the manuscript submitted to Acta Mater. [2005Cao1].

2.2 The Use of the CSA for the Calculation of Coherent IPB Energy

In view of the relative computational simplicity of the CSA and the fact that it is able to calculate binary and now ternary phase diagrams not only for prototype ones such as Cu-Ag-Au but also for the real system Ni-Al-Cr, we have been exploring the use of the CSA to calculate coherent IPB energies of the prototype Cu-Au binary. Our motivation was: if this approach were shown to be a suitable one, we could then extend the use of this approach to calculate IPB energies, for instance, between γ and γ' in multicomponent Ni-based superalloys. These quantities are essential for describing microstructure evolution when an alloy undergoes thermal treatment using kinetic modeling such as the phase-field approach. We first used the CSA to calculate the IPB energies of binary immiscible alloys and then those between the prototype fcc-(Cu, Au) and the ordered $L1_2$-(Cu_3Au) phases. The calculated results for the immiscible binary case agree with those obtained by Kikuch and Chen [95Kik] using the CVM but deviate from those obtained by Lee and Aaronson [80Lee]

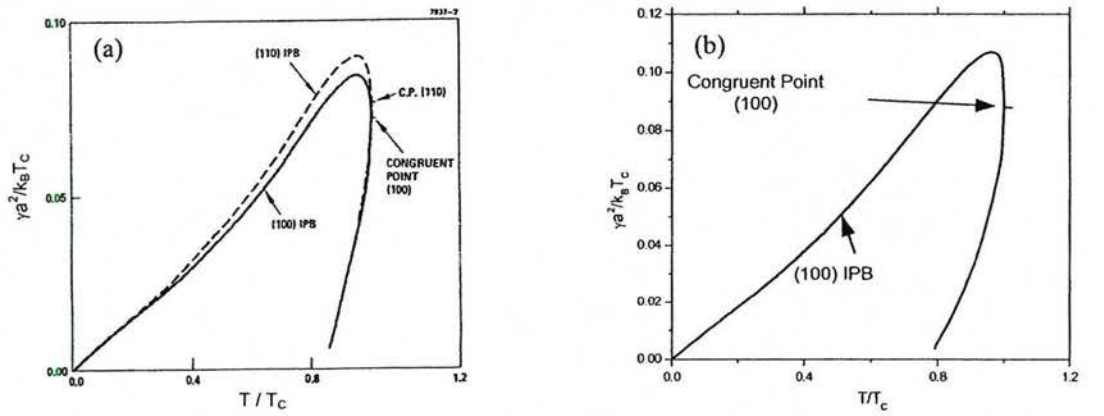

Figure 8 Calculated coherent IPB energies of the fcc-(Cu, Au) and $L1_2$-Cu_3Au phases using the tetrahedron approximation: (a) CVM-Calculation for the (100) & (110) planes, (b) CSA calculation for (100) planes.

using a regular solution model. A manuscript summarizing the results of our study has been submitted to Scripta Materialia for publication [2005Cao2]. We will present the results obtained for the latter case as given below.

Comparisons of the CSA-calculated coherent IPB energies between the fcc-(Cu, Au) and the $L1_2$-(Cu_3Au) phases with the CVM-calculated values [79Kik] are presented in Figs. 5(a) and (b). In both cases the tetrahedron approximation was used. Our calculation was carried out following the approach of Kikuchi and Cahn but using the CSA instead of the CVM. The pair exchange energy W for the CSA calculation was taken from Oates et al. [99Oat]. As shown in Fig. 5(b) the CSA-calculated IPB energies for the (100) plane are in accord with those given in Fig. 5(a) calculated by Kikuchi and Cahn from the congruent point down to low

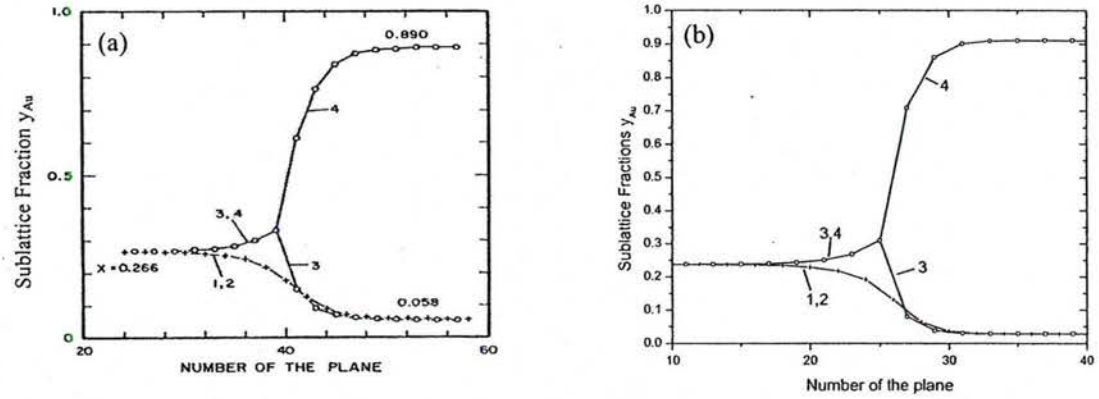

Figure 6 Calculated concentration profile for the (100) IPB at the congruent point: (a) CVM and (b) CSA.

temperatures. As also shown in Fig. 6(b), the CSA-calculated concentration profile for the (100) IPB between these two phases at the congruent point are also in accord with the CVM-calculated values shown in Fig. 6(a). These results led us to believe that the CSA could be used to calculate IPB energies and should be explored further. As noted previously [79Kik, 96Ast1], the vanishing of the calculated IPB energy at 0K using the tetrahedron approximation is due to the neglect of the longer-range interaction in the lattice. Using the tetrahedron-octahedron approximation of the CVM (TO-CVM), expressed in terms of the parameter $\alpha = W_2/W_1$ for α = -0.1 and -1.0, Asta [96Ast1] calculated the phase diagrams of

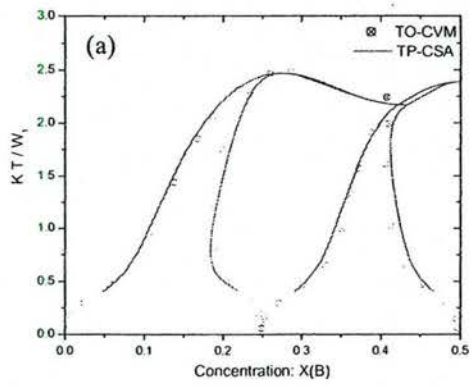

Figure 7 (a) Calculated prototype Cu-Au phase diagram with α = -0.1 with the TO-CVM calculated values shown as discrete points [96Ast1] and the TP-CSA values as smoothed curves.

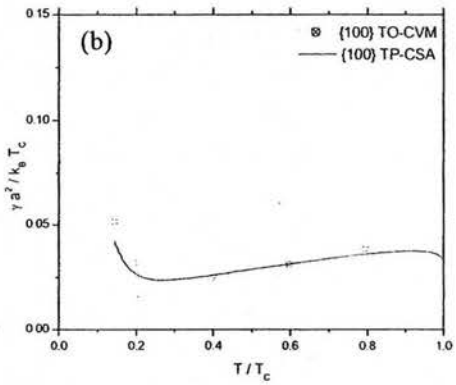

Figure 7 (b) Calculated IPB energies between the fcc and $L1_2$ phases with α = -0.1. The TO-CVM calculated values are shown as discrete points [96Ast1] and TP-CSA values as a smoothed curve.

the prototype Cu-Au binary and then the coherent IPB energies between the fcc-(Cu,Au) and the $L1_2$-(Cu_3Au) phases. The terms W_2 and W_1 denote the next nearest neighbor and the nearest neighbor pair exchange energies, respectively. Figures 7(a) and (b) show the TO-CVM and TP-CSA calculated phase diagram and coherent IPB energies between the fcc-(Cu, Au) and $L1_2$-Cu_3Au phases for the (100) planes. The TO-CVM calculated values were taken from Asta [96Ast1] and shown in these figures as discrete points. As shown in Fig. 7(b) the coherent IPB energy at 0K is finite and decreases first with increasing temperature and then change slowly with further increases in temperatures. We used the tetrahedron-pair approximation of the CSA (TP-CSA) to calculate the phase diagram and coherent IPB energies [99Vak]. Our TP-CSA calculated reduced temperatures expressed as a function of composition as shown in Fig. 7(a) represented by smoothed curves are in accord with the TO-CVM calculated values. Likewise, the TP-CSA calculated coherent IPB energies given in Fig. 7(b) shown as a smoothed curve is in accord with the TO-CVM calculated results. We did not calculate the values down to 0K due to numerical difficulties, which will be resolved in the near future. Nevertheless, the fact that the calculated values are in reasonable accord with the TO-CVM calculated results [96Ast1] is encouraging.

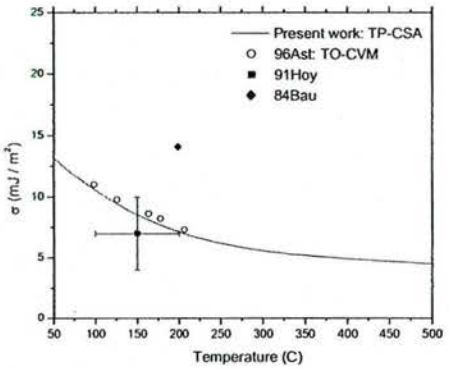

Figure 8 (a) Comparisons of TP-CSA-calculated coherent IPB energies between fcc-(Al) and $L1_2$-Al_3Li with the TO-CVM values and the experimental data [91Hoy, 84Bau].

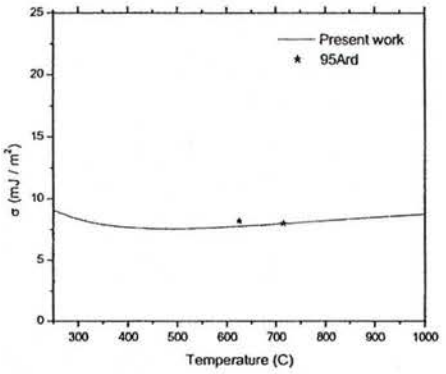

Figure 8 (b) Comparisons of TP-CSA-calculated coherent IPB energies between γ and γ' in Ni-Al with experimental data [90Mar, 95Ard].

We next extended the TP-CSA to calculate the coherent IPB energies between the fcc and $L1_2$ phases in two real alloy systems, i.e. Al-Al_3Li and Ni-Al. As shown in Fig. 8(a) the TP-CSA calculated IPB energies are in accord with the TO-CVM calculated values [96Ast]. Within the uncertainties of the measurements, there is agreement between the calculated values and the experimental data of Hoyt and Spooner [91Hoy] and Baumann and Williams [84Bau]. Figure 8(b) shows that the TP-CSA calculated IPB energies between γ and γ' in Ni-Al are in accord with the experimental values of Ardell [95Ard]. Ardell re-evaluated the data of Marsh and Chen [90Mar] and obtained values in the range of 2 mJ/m^2 but not shown in this figure. It is worth noting that Dr. Chris Woodward of the AFML, Dayton, OH [2004Woo] shared his calculation of IPB energies between γ and γ' in Ni-Al with us. He used a "first principles" cluster expansion method coupled with Monte Carlo calculations to estimate the interfacial width and excess free energy in γ and γ' in Ni-Al. For temperatures in the range of experimental measurements (see Figure 8(b)) his calculated IPB energies are in good agreement with our estimates, and with the available results from experimental measurements. These results indicate that the CSA, computationally less demanding than the CVM, offers an alternative and perhaps practical approach to calculate (or estimate) coherent IPB energies for γ and γ' in other Ni binaries and even to higher order alloys of practical importance.

3.0 Proposed Study

We propose to carry out the following studies: (1a) to apply the CSA to the fcc phases in quaternary Ni-based alloy systems such as Ni-Al-Cr-Re including its constituent ternaries, (1b) to first develop a thermodynamic description of ternary Ni-Al-Pt using the traditional Calphad approach in terms of experimental data in the literature and additional data to be determined in the proposed study and then to apply the CSA to the fcc phases for this ternary in a manner as proposed in (1a), (1c) to obtain a thermodynamic description of the quaternary Ni-Al-Cr-Pt system via extrapolation with experimental validation, and (2) to apply the CSA to calculate coherent IPB energies between γ and γ' in higher order Ni-based alloys such as Ni-Al-Cr.

3.1 Application of the CSA to Calculate Phase diagrams of Quaternary Ni-Al-Cr-based Alloys

As presented in **Section 2.1**, we have successfully applied the CSA to the fcc phases in the calculation of the ternary Ni-Al-Cr system [2005Cao1]. We propose to extend the CSA-calculation from ternaries to quaternaries. The CSA-calculation means that the CSA is used for the fcc phases but the thermodynamic models used for all other phases are the ones used in the traditional Calphad approach. We select quaternary Ni-Al-Cr-Re as a model system for our proposed study. This system is selected for the following reasons: (i) it is an important quaternary system for nickel-based superalloys since the addition of Re improves the mechanical properties of Ni-based superalloys [93Qui], (ii) extensive phase equilibrium data exist between γ and γ' in Ni-Al-Cr-Re [94Miy], and (iii) a thermodynamic description obtained using the traditional Calphad methodology is available [98Hua]. Moreover, the calculated compositions of γ in equilibrium with γ' in this quaternary using this description [98Hua] are in accord with experimental data [94Miy]. The six constituent binaries of this quaternary are Ni-Al, Ni-Cr, Ni-Re, Al-Cr, Al-Re and Cr-Re and the four constituent ternaries are Ni-Al-Cr, Ni-Al-Re, Ni-Cr-Re and Al-Cr-Re. Out of the six binaries, CSA-descriptions are available for Ni-Al, Ni-Cr and Al-Cr [2003Zha, 2005Cao1]. Accordingly, we need only to develop the CSA-descriptions for the other three Re-containing binaries. Since the CSA-description is only available for the Ni-Al-Cr system, we will have to develop CSA-descriptions for the other three ternaries. Based on these descriptions, we will obtain a description for this quaternary via extrapolation. We will then calculated quaternary phase equilibria using this CSA description and anticipate that the calculation will be in good accord with experimental data [94Miy]. This statement is made based on our experience when we obtained the CSA-descriptions of binary Ni-Al and ternary Ni-Al-Cr using the descriptions obtained by the traditional Calphad method as the starting points. When this is demonstrated, we could conclude that this approach using the CSA to describe the fcc phases *represents an advancement to calculate multicomponent phase diagrams of the technologically important Ni-based alloys*. Yet fewer thermodynamic parameters are needed using the CSA than the Bragg-Williams model. Using the CSA-description, we can explore the calculation of a number of metastable phase diagrams. Moreover, we will have more confidence in using this type of thermodynamic descriptions to calculate thermodynamic driving forces for phase transformation, leading to the prediction of microstructure and ultimately the mechanical behaviors of the materials.

3.2 Thermodynamic Description of Ni-Al-Pt Using a Combined Computational/Experimental Approach

There has been intense recent interest in the phase stability of multicomponent Ni-based alloys containing Pt for the prevention of oxidizing Ni-based superalloys at high temperatures. Since Ni-Al-Pt is a key ternary for these multicomponent alloys, it is important to develop a thermodynamic description of this ternary first in terms of ternary experimental data and thermodynamic descriptions of the constituent binaries. An earlier 1060°C isotherm presented by Batzner [90Bat] and Jackson and Rairden [78Jac] was estimated based on the experimental observation of Jackson and Rairden [77Jac]. However, very recently, Wang et al. [2005Wan] and Hayasha et al. [2005Hay] have determined the solid-state phase equilibria of Ni-Al-Pt at 1100 and 1150°C. As shown in Fig. 9, several of the binary intermetallic phases exhibit extensive solubilities. The phase equilibria at 1150°C differ little from those at 1100°C shown in Fig. 9. It is interesting to note that the $L1_0$ phase denoted by the authors as α-NiPt(Al) exists over a wide range of homogeneity. This phase is in equilibrium with γ', γ and β. However, it is not stable either in binary Ni-Al or Pt-Al. As shown in Fig. 4(a) a CSA-calculated *metastable phase diagram of Ni-Al based on the fcc phase shows the existence of the $L1_0$ phase at 50 at% Al with appreciable range of homogeneity*. This ternary isotherm shown in Fig. 9 indicates that the metastable $L1_0$ phase in Ni-Al becomes stable with the addition of Pt. It is now clear from Fig. 9 that additional phase diagram information is needed before we can obtain a reliable thermodynamic description for this ternary. For instance there is no information on either the solid/liquid equilibria or the equilibria between the $L1_0$ phase and other Pt-rich phases and the Pt-rich γ-solid solution. Our combined computational/experimental approach to obtain a thermodynamic description of a ternary such as Ni-Al-Pt is given below.

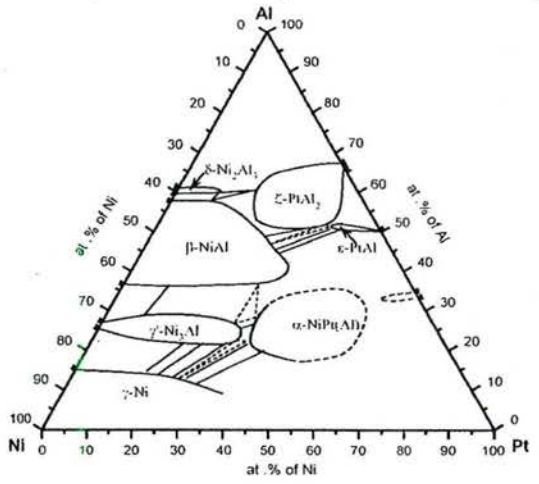

Figure 9 1100°C isotherm [2005Wan, 2005Hay]

Thermodynamic descriptions are available in the literature for all three constituent binaries of Ni-Al-Pt: Ni-Al [98Hua], Al-Pt [2000Wu], and Ni-Pt [85Dah]. For Al-Pt, we will initially adopt the description of Wu and Jin [2000Wu]. But it is likely that we will have to improve this description based on our past experience. On the other hand, since the published description of Ni-Pt is based on the CVM for the coherent prototype fcc phase diagram, we will develop a thermodynamic description of this binary using the traditional Calphad approach in terms of the data published by these investigators in addition to those given in an earlier extensive review by Nash and Singleton [89Nas]. On the basis of these binary descriptions together with the phase equilibria shown in Fig. 9, we will attempt to obtain a preliminary description of this ternary using the traditional Calphad approach. Based on this description we will calculate several phase diagrams; on basis of which, we can identify a minimum number of alloys for additional experimental investigation. These new data will allow us to obtain an improved thermodynamic description. Often it is necessary to go through more than one cycle to obtain a satisfactory ternary description. In addition, we may also have to go back to improve some of the binary descriptions. We have indeed used such a combined computational/experimental approach to determine the phase diagrams of Mo-Si-B-

Ti and two of its constituent ternaries [2004Yan, 2005Yan, 2005Yan1]. Once we are satisfied with this ternary description obtained in the traditional approach, we will then apply the CSA model to the fcc phases to obtain a CSA-description as presented in **Section 2.1**.

3.3 Thermodynamic Description of Ni-Al-Cr-Pt by Extrapolation with Experimental Validation

From a practical point of view, it is desirable to obtain a thermodynamic description of the quaternary Ni-Al-Cr-Pt. However, to go through a process in obtaining a description of Ni-Al-Cr-Pt as we just presented for Ni-Al-Pt would take tremendous amount of effort. An alternative and more realistic approach is to obtain descriptions of the other two ternaries by extrapolation of the binary descriptions since a description for Ni-Al-Cr is available and a description of Ni-Al-Pt will be developed. On the basis of the four constituent ternaries, two Ni-Al ternaries modeled and the other two extrapolated, we can go ahead to obtain a description of the quaternary. We will next carry out few experiments on Ni-rich alloys either to validate the description so obtained or to realize the uncertainties involved.

3.4 Use of the CSA to Calculate IPB Energies between γ and γ' in Ternary Ni-Al-Cr Alloys

We plan to first calculate IPB energies between γ and γ' in binaries for different atomic planes such as (111) using the same approach as presented in **Section 2.2** and then extend the calculation to ternaries such as Ni-Al-Cr. We choose this ternary since it is one of the most important ternaries for Ni-based superalloys.

3.5 Experimental Investigations

We will use Ni-Al-Pt as an example to illustrate the approach used to determine phase equilibria when such data are either non-existing or judged to be unreliable. As given in **Section 3.2**, there is no experimental information on the solid/liquid phase equilibria for this ternary and the data given in Fig. 9 for the solid-state phase equilibria are incomplete. Before doing any experiments, we will obtain a preliminary thermodynamic description of Ni-Al-Pt based on descriptions of the constituent binaries and available ternary experimental data. This description will allow us to calculate a liquidus projection and isothermal sections. On the basis of the calculated phase diagrams, we can select a limited number of alloys for solidification and isothermal annealing studies. An analysis of the microstructures of the solidified samples will provide information on the primary phases of solidification and a similar analysis of the isothermally annealed samples solid-state phase equilibria. With these additional experimental data, we can make an improved thermodynamic description that in turn will allow us to identify another set of limited number of additional new alloys for experimental investigation. When we developed a thermodynamic description of quaternary Mo-Si-Bo-Ti, it took us two cycles before we obtained a reliable description for that system [2004Yan, 2005Yan]. It is our expectation that this will be the case for Ni-Al-Pt. It is noteworthy to point out that we have communicated with Prof. B. Gleeson of the Iowa State University with respect to his experimental effort of Ni-Al-Pt. For instance, we have two preprints from him [2005Hay, 2005Wan] as noted in **Section 3.2** (see Fig 9). We will continue to interact with him so that we will work in a synergetic manner to advance an

understanding of the phase stability of this ternary. In other words, we will make absolutely sure that our respective efforts are absolutely complementary!

We will use SEM to characterize the microstructure of the as-solidified alloys. The phases presented in the as-solidified alloys can be determined by X-ray diffraction (XRD) and their compositions by electron probe microanalysis (EPMA). In case that the fraction of a certain phase is too small to be detected by X-ray diffraction, it can be detected by Electron BackScattered Diffraction EBSD. This technique has the capability to detect the crystal structure of an individual phase particle (>1μm). If proved necessary, we will use TEM for phase characterization. Moreover, the as-solidified or cast alloys can be annealed at a fixed temperature such as 1100°C to achieve equilibrium. The phases in the annealed alloys can be also characterized by XRD and the compositions of the co-existing phases can be determined by EPMA. We have had ample experience in binary and higher order phase diagram investigations [e.g. 98Lia, 2001Din, 2002Din, 2004Yan, 2005Yan, 2005Yan1, 2005Yan2].

Alloys for experimental investigation are made first by arc melting of high purity Ni, Al and Pt for the case of ternary Ni-Al-Pt, followed by heat-treatment at a specified temperature to achieve equilibrium. Although we have taken this ternary system to illustrate the general approach used to determine phase equilibria, the same approach can be used to determine the phase diagrams of binary and higher order systems [e.g., 2001Din, 2002Din, 2004Yan, 2005Yan]. In addition, we have had extensive experience in carrying out diffusion couple measurements, differential thermal analysis (DTA) and differential scanning calorimetry (DSC). When needed, we will use these tools to further establish specific types of phase equilibria. For instance, we have recently used a combinatorial approach, employing diffusion triplets [2001Zha2], to determine an isothermal phase diagram of ternary Mo-Re-Si [2005Yan2] and will use it again when appropriate for specific ternary systems. A list of the equipments/apparatus and characterization tools at our disposal are given in **Section 4.0: Experimental Facilities**.

4.0 Experimental Facilities

Our laboratories are equipped to carry out the investigations proposed here. A list of equipment available in the laboratories of Prof. Chang's research group is given first and then the general facilities available in the Department of Materials Science & Engineering, the Center of Materials Sciences in the College of Engineering as well as facilities on the campus of the University of Wisconsin, Madison, WI, are also given.

4.1 Experimental Equipments and Instruments in Prof. Y. A. Chang's Research group

(a) An arc-melter for making metal alloys. We have set up a state-of-the-art arc-melting furnace purchased from Centorr. Since this melter is under our exclusive control, we have been able to prepare quality alloys, from Al alloys to high melting alloys and intermetallic compounds. We have designed and fabricated a new copper hearth for this arc-melter, so that we can cast intermetallic specimens having a diameter of 1/4" (~6 mm) for diffusion couple specimens. The ultra-high-purity argon used is further gettered using a titanium deoxidizing furnace similar to that used in the RTA furnace as described in (b).

(b) A Deltec high-temperature (1700°C) furnace. It has been used for homogenizing high-temperature alloys under the flow of ultra-high purity argon.

(c) Numerous other furnaces in our laboratory with maximum temperature capabilities of 1100-1500°C.

(d) A Perkin-Elmer DSC-7 Differential Scanning Calorimeter. We have used this instrument to measure the thermal peaks of lots of films as a function of thermal annealing. This unit is being modified to interface with modern computers and improved so that it will be able to run under isothermal conditions. This improvement will enhance our capability in studying the kinetics of microstructural and structural changes when intermetallic thin-films are subjected to thermal annealing.

(e) A dedicated vacuum system for encapsulating samples for bulk diffusion couple studies, as well as another dedicated vacuum system utilizing a turbo-pump backed by a mechanical pump for encapsulating thin-film diffusion couples for heat treatment. The latter system is capable of achieving a much better vacuum, i.e., 10^{-7} Torr in about an hour.

(f) A Leco oxygen analyzer for determining the oxygen concentration of metals and alloys. We have used this technique routinely to determine the oxygen concentrations in the aluminides prepared in our laboratory.

(g) A dry box manufactured by Vacuum/Atmosphere Co. for providing an inert atmosphere chamber with an oxygen concentration of less than 5 ppm.

(h) Two cryo-pumped sputter deposition systems are available to make a variety of thin-films. Some specialized highlights include: up to three targets co-focal sputtering with simultaneous substrate rotation and heating, deposition angle control, RF and DC magnetron sputtering, and multiple gas atmosphere control.

(i) A Multipulse 310 Rapid Thermal Annealing (RTA) furnace. This furnace is capable of ramping from ambient to temperatures up to 1000°C in seconds. The furnace operates in Ti deoxidized, ultra-high-purity Ar atmosphere and includes multistep computer control.

(j) An Accupyc1330 density measurement unit from Micromeritics Co. It can measure density of solid sample with accuracy of 0.0001 g/cm^3. Lots of vacancy concentration experiments were performed in this system by means of its high accuracy and sensitivity.

(k) A slow wire saw. It is good for cutting the brittle materials, such as silicon wafer.

(l) A MultiPrep™ System from Allied High Tech. Inc. The MultiPrep™ System enables precise semiautomatic sample preparation of a wide range of materials for microscopic (optical, SEM, TEM, AFM, etc.) evaluation. Capabilities include parallel polishing, precise angle polishing, site-specific polishing or any combination thereof. It provides reproducible sample results by elimination inconsistencies between users, regardless of their skills.

(m) A Rotopol-2 Integrated Grinding and Polishing sample preparation equipment from Struers Co. Grinding/polishing machine with two 250 mm diameter Discs for manual or automatic preparation of materialographic specimens has following features: ergonomical

design, finger-touch controls, and electronic control of all functions. Three different models can meet all demands. Semi-automatic or automatic specimen mover can be mounted and prepared for recirculation unit.

(n) An Electrical Property Measurement System, including Signatone H100 series four-probe station, Keithley 236 Source Measure Unit Mode590 CV analyzer and Computer Controlling System. It has the capabilities to do typical four-probe electrical properties measurement.

(o) A Directional Solidification Apparatus System, consisting a sample preparation furnace and directional solidification apparatus. It is well established, produces uniform microstructures and allows better control of solidification conditions.

(p) A mini Arc Melting System from Edmund Buhler Co. MAM-1 is well suited for melting and alloying of small quantities (up to approximate 15g) in an extremely pure argon atmosphere after the melting chamber was pumped into high vacuum condition. It has special cold crucible for melting rod-shaped samples. With this special crucible the molten sample can be cast into rods with variant diameters, from 0.5mm to 5mm.

4.2 Experimental Facilities available in the Department of Materials Science and Engineering and the Center of Materials Science

1. Furnaces, HIP and Presses

An IPS Eagle HIP unit has been used for making samples for diffusion couples such as Ni/Mn. The HIP is capable of attaining pressures to 40k Psi and temperature to 1800°C using Mo heating elements. Higher temperatures can be attained using graphite heating elements.

A high-temperature (~1500°C or higher for limited time) hot press operated either under vacuum or in an inert gas atmosphere has been recently modified by us for fabricating diffusion couples such as Ni/Mn and casting Al alloys.

An Edmond Buehler ultra-rapid quench apparatus is available which may be used to prepare rapidly solidified samples when needed.

2. Sample Preparation

There are numerous grinding and polishing machines, which can be used for optical microscopy, SEM, and TEM sample preparation.

There are several complete metallographic facilities such as a Zeiss Ultraphot, a Leitz metallograph, a Nikkon metallograph, and numerous Olympus-metallographs for micro- and macro-metallography.

Several Ion Milling systems, including Fischione 1010 with low angle milling condition and complete computer control and Ion Tech Mill, have being used for TEM and STEM sample preparation.

A state-of-the-art FIB/SEM platform, which can perform sample preparation (for SEM, TEM, AFM, Auger, SIMS, Atom Probe, etc), and milling/deposition for nanotechnology, will be ready for use soon.

We also have several vacuum coating systems, like Denton High Vacuum Coating System and VCR Ion Beam Coating System.

3. Electron Microscopy (SEM and TEM)

A dedicated analytical STEM (VG HB501) with 5Å resolution can perform STEM and EELS study with full support of image processing and spectroscopy simulation capability. A JEOL 200 CX TEM/STEM has features like 5 Å resolution, full range of sample holder including heating, cooling and double tilt, EDS and micro-diffraction. A high-resolution Phillips CM200 Ultra Twin TEM with better than 2Å resolution, light element EDS, and full image processing/analysis capabilities. A LEO 912 field emission microscope featuring 4Å (spot to spot) resolution with energy filter option can be used for both imaging and chemical analysis.

JEOL JSM 6100 SEM equipped with SE and BSE detector. A state-of-the-art LEO 1530 FESEM, featuring field emission gun, high magnification up to 200KX, light element EDS detector, BSE detector, Electron Backscattered Kikuchi Pattern detector.

4. X-Ray Diffraction System

Three Philips machines with computer-automated diffractometer can be used for the study of bulk sample, such as crystal structure and lattice parameter, etc.

An Inel diffraction system with a CPS 120 curved detector, which can collect the signal from 0~120° simultaneously, which make the normal powder diffraction done in several minutes.

A STOE system with four-circle configuration and high temperature furnace can be used for the study of both bulk and thin film sample, such as thermal expansion, texture, and epitaxy structure, etc. The main features include standard Bragg-Brentano goniometer, focused beam transmission goniometer, minimum step size 0.001°, multiple stages to accommodate many specimen types, high temperature furnaces for phase transition studies.

A Hi-Star 2-D system which is equipped with a two dimensional detector, can carry out excellent jobs for fast and accurate texture and epitaxy study of thin films.

A Panalytical X'Pert MRD system, one of the most flexible systems available for X-ray diffraction studies for advanced materials science and nanotechnology. It can handle a wide range of applications, and is especially suitable for thin film analysis applications such as, rocking curve analysis and reciprocal space mapping, X-Ray scattering capability to reveal interface roughness information and high resolution diffraction capability to study superlattice structure, texture analysis, and residual stress.

5. Surface Science Equipment

An Auger electron Spectroscopy unit PHI 670 SAM is capable of elemental surface analysis, multi-point analysis, and small feature analysis. The Argon Ion sputter etching gun enables the system to perform depth profile. A number of standards are available to allow precise

compositional analysis (0.5at% detection limit) of phases in thin films as well as the measurement of the thickness of phases.

In addition, we also have an Angle-Resolved Small Area ESCA/XPS System Model 5400, with dual anode X-Ray source (Al, Mg), which can perform element surface analysis and chemical status analysis by the peak and shape shift of the XPS spectrum. The argon Ion sputter etching gun enables system to carry out composition depth profile.

The Digital Instrument Multimode SPM with NanoScope IV, which is capable of performing the full range of atomic force microscopy (AFM) technique to measure surface characteristics like topography, elasticity, friction, adhesion, and magnetic/electrical fields. The short mechanical path length between probe tip and sample enables very fast scan rates with utmost precision.

6. Composition Analysis

Inductively coupled plasma mass spectrometry (ICP-MS) for composition analysis of solder samples (Soil Science Laboratory),

The faculty of the Department of Geology and our faculty in Materials Science and Engineering have jointly operated a CAMECA electron probe model no. SX50, which provides compositional and image analysis. We have been using this instrument routinely to determine concentration profiles in diffusion couples as well as in solidified samples.

7. Mechanical property Analysis

A Micromet II and Macromet II units from Buehler Co. are capable of micro-hardness measurement. An Instron machine is used for mechanical property experiment, such as tensile, compress measurement.

A Nano Instruments Nano Indenter-II unit, (Department of Nuclear Engineering and Engineering Physics), is capable of performing hardness, elastic modulus, and fracture toughness analysis, etc.

The College of Engineering has supporting personnel in machining and electronics shops. In addition, the Department has three specialists who are responsible for maintaining electronics and related equipment. There is a glass blower who operates a private business 10 miles away from the City of Madison. He comes to campus regularly to do work for research personnel.

5.0 References Cited

[38Sho] W. Shockley, J. Chem. Phys., 1938, 6, 130.
[47Yan] C. N. Yang and Y. Li, Chin. J. Phys., 1947, 7, 59.
[48Red] O. Redlich and A. Kister, Ind. Eng. Chem., 1948, 40,345.
[51Kik] R. Kikuchi, Phys. Rev., 1951, 81, 988.
[74Kik] R. Kikuchi and C. M. Van Baal, Script. Mater., 1974, 8, 425.
[77Jac] M. R. Jackson and J. R. Rairden, Metall. Trans., 1977, 8A, 453.
[78Jac] M. R. Jackson and J. R. Rairden, in NBS Special Publication, SP-496, Applications of Phase diagrams in Metallurgy and Ceramics, Proceedings of Workshop, Gaithersburgg, 1978, 423-439.
[78San] J. M. Sanchez and D. de Fontaine, Phys. Rev., 1978, 17B, 1926.
[79deF] D. de Fontaine, "Configurational Thermodynamics of Solid Solutions" in Solid State Physics, 1979, 34, 73.
[79Kik] R. Kikuchi and J. W. Cahn, Acta Metall., 1979, 27, 1337-1353.
[80Kik] R. Kikuchi, R. Sanchez, D. de Fontaine, H. Yamauchi, Acta Mater., 1980, 28, 651.
[80Lee] Y. W. Lee and H. I. Aaronson, Acta Metall, 1980, 28, 439-547.
[83Och] S. Ochiai, Y. Oya, T. Suzuki, Bull P M E (T I T) 1983, 52,1.
[84Bau] S. F. Baumann and D. B. Williams, Scripta Metall. 1984, 18, 611.
[85Dah] C.E. Dahmani and M.C. Cadeville, Phys. Rev. Letters, 1985, 55(11), 1208-1211.
[86And] J.O Anderson, A. f. Guillermet, M. Hillert, B, Jason, and B. Sundman, Acta Metall., 1986, 34, 437.
[89Cho] K.-C. Chou and Y. A. Chang, "A Study of Ternary Geometrical Models", Ber. Bunsenges. Phys. Chem., 1989, 93, 735.
[89Hon] Y. M. Hong, H. Nakayima, Y, Mishima, and T. Suzuki, ISIJ International, 1989, 29, 78.
[89Nas] P. Nash and M.F. Singleton, Bull. Alloy Phase Diagrams, 1989, 10, 258-62, 307-8.
[90Bat] C. Batzner, in Phase Diagrams of Ternary Nickel Alloys, VCH, 1990. 449.
[90Mar] C. Marsh and H. Chen, Acta Metall., 1990, 38, 2287.
[91Hoy] J. J. Hoyt and S. Spooner, Acta Metall. 1991, 39, 689.
[92Pas] A. Pasture, K. Colinet, A. T. Paxton and M. J. Schilfgaarde, Phys. Condens. Matter, 1992, 4, 945.
[93Qui] R. J. Quigg, High Temp. Mater. Process, 1993, 11, 247-254.
[94deF] D. de Fontaine, "Cluster Approach to Order-Disorder Transformations in Alloys" in Solid State Physics, 1994, 47, 33-176.
[94Hua] W. Huang and Y. A. Chang, Mater. Sci. Engin, 1999, A259, 110-119.
[94Miy] S. Miyazaki, Y. Murata and M. Morinaga, Tetsu-To-Hagane, 1994, 80, 166-171.
[95Ard] A. J. Ardell, Interface Science, 1995, 3 119.
[95Kik] R. Kikuchi and L.-Q. Chen, NanoStructured Mater., 1995, 5, 257-268.
[96Ast] M. Asta, Acta Mater., 1996, 44, 4131-4136.
[96Ast1] M. Asta, "Thermodynamic Properties of Coherent Interphase Boundaries in fcc Substitutional Alloys", in Theory and Applications of the Cluster Variation method and Path Probability Methods (Eds: J. L. Moran-Lopez and J. M Sanchez), Plenum Press, New York, 1996, 237-254.
[96Oat] W. A. Oates and H. Wenzl, Scripta Mater., 1996, 35, 623.
[98Hua] W. Huang and Y. A. Chang, Intermetallics, 1998, 6, 487-498; Corrigendum: Intermetallics, 1999, 7, 625-626.
[98Lia] Liang, H., "Thermodynamic Modeling and Experimental Investigation of the Al-Cu-Mg-Zn Quaternary System", Ph. D. Thesis, University of Wisconsin, Madison, WI, 1996.
[98Sun] B. Sundman, S. G. Fries and W. A. Oates, CALPHAD, 1998, 22, 355.
[99Oat] W. A. Oates, F. Zhang, S.-L. Chen and Y. A. Chang, Phys. Rev., 1999, 59B, 11221-11225.
[99Vak] V. G. Vaks and G. D. Samolyuk, J. Expt. Theor. Physics, 1999, 88, 89-100.
[2000Wu] K. Wu and Z. Jin, J. Phase Equilibria, 2000, 21, 221-226.
[2001Che] S.-L. Chen, S. Daniel, F. Zhang, Y. A. Chang, W. A. Oates and R. Schmid-Fetzer, J. Phase Equilibria, 2001, 22, 373-378.

[2001Din] L. Ding, "Experimental Investigation of Phase Equilibria and Interdiffusion coefficients in Ni-Mn System", M.S. Thesis, University of Wisconsin Madison, WI, 2001.
[2001Zha] J. Zhang, W. A. Oates, F. Zhang, S.-L. Chen, K.-C. Chou and Y, A. Chang, Intermetallics, 2001, 9, 5-8.
[2001Zha1]F. Zhang, W. A. Oates, S.-L. Chen, and Y. A. Chang, "Cluster-Site Approximation (CSA) Calculation of Phase Diagrams," in High Temperature Corrosion and Materials Chemistry III (Eds.: M. McNallan and E. Opila) The Electrochemical Society, Pennington, NJ, 2001, 12, pp. 241-252.
[2001Zha2]J.-C. Zhao, J. Mater. Res., 2001, 16, 1565.
[2002Che] S.-L. Chen, S. Daniel, F. Zhang, Y. A. Chang, X.-Y. Yan, F.-Y. Xie, R. Schmid-Fetzer and W. A. Oates, CALPHAD, 2002, 26, 175-188.
[2002Din] L. Ding, P. Ladwig, X.-Y. Yan and Y. A. Chang, Appl. Phys. Lett., 2002, 80, 1186-1188.
[2003Che] S.-L. Chen, F. Zhang, S. Daniel. F.-X. Xie, X.-Y. Yan, Y. A. Chang, R. Schmid-Fetzer, and W. A. Oates, JOM, 2003, 55, December, 48-52.
[2003Zha] F. Zhang, Y. Du, W. A. Oates, S.-L. Chen, and Y. A. Chang, Acta Mater, 2003, 51, 207-216.
[2004Cha] Y. A. Chang, S.-L. Chen, F. Zhang, X.-Y. Yan, F.-Y. Xie , R. Schmid-Fetzer, and W. A. Oates, "Phase Diagram Calculation: Past, Present and Future", Prog. Mater. Science, 2004, 49, 313-345.
[2004Woo] C. Woodward, AMRL, Dayton, OH, private communication, 2004.
[2004Yan] Y. Yang, Ph.D. Thesis, "Thermodynamic modeling and experimental investigation of the Mo-Si-B-Ti quaternary system", University of Wisconsin, Madison, WI, 2004.
[2005Cao] W. Cao, Y. A. Chang, J. Zhu, S.-L. Chen and W. A. Oates, Acta Mater., 2005, 53, 331-335.
[2005Cao1] W. Cao, J. Zhu, Y. Yang, F. Zhang, S.-L. Chen, W. A. Oates and Y. A. Chang, Acta Mater., 2005, under review.
[2005Cao2] W. Cao, J. Zhu, Y. Yang, W. A. Oates and Y. A. Chang, "Thermodynamic Stability of Co/Cu Multilayered Nanostructures", Script. Mater., 2005, under review.
[2005Hay] S. Hayashi, S. I. ford, D. J. Young, D. J. Sordert, M. F. Besser and B. Gleeson, "α-NiPt(Al) and Phase Equilibria in the Ni-Al-Pt System at 1150°C", 2005, submitted for publication. Prof. B. Gleeson sent us a copy of this pre-print.
[2005Wan] W. Wang, S. Hayashi, D. Sordert and B. Gleeson, "Phase Equilibria in the Ni-Al-Pt system at 1100°C", 2005, submitted for publication. Prof. B. Gleeson sent us a copy of this pre-print.
[2005Yan] Y. Yang, Y.A. Chang, L. Tan and W. Cao, Acta Mater, 2005, 53, 1711-1720.
[2005Yan1]Y. Yang, Y.A. Chang and L. Tan, Intermetallics, 2005, in press.
[2005Yan2]Y. Yang and Y. A. Chang, "Mapping the Phase equilibria of the Mo-Re-Si using diffusion multiples", 2005, in preparation